

## AC Operation of a D-<sup>3</sup>He Tokamak Fusion Reactor

Mitarai, Osamu

Department of Electrical Engineering, Kumamoto Institute of Technology

<https://hdl.handle.net/2324/1546614>

---

出版情報 : 7th International Conference on Emerging Nuclear Energy Systems, pp.12-15, 1993

バージョン :

権利関係 :

# AC OPERATION OF A D-<sup>3</sup>He TOKAMAK FUSION REACTOR

Osamu MITARAI

Department of Electrical Engineering,  
Kumamoto Institute of Technology,  
Ikeda 4-22-1, Kumamoto 860 Japan

## Abstract

We propose an inductive alternating current (AC) D-<sup>3</sup>He tokamak reactor ( $R=9.5$  m,  $a=2.8$  m,  $B_t=10$  T and  $I_p=53.6$  MA), operated in the first stability regime, with a small current-drive power  $\sim 500$  kW in the plasma side, and  $\sim 2$  MW in the transformer side. The high electron temperature  $T_e(0) \sim 62.5$  keV together with the high bootstrap current fraction  $> 70\%$  decreases the plasma resistance (to less than  $1$  n $\Omega$ ) and the loop voltage ( $\sim 10$  mV range), and then prolongs the pulse length to more than 15 hours. The ignition characteristics of a D-<sup>3</sup>He tokamak reactor are analyzed by the operation path method on the  $P_{ht}\tau_E^2$ -T plane and POPCON for different confinement scalings.

## 1. Introduction

The steady-state operation is the best operation scenario in the tokamak reactor. However, the non-inductive current drive schemes, such as neutral beam and radio-frequency current drive studied so far, are not proven yet to be effective in an ignited regime due to the penetration problem of the neutral beam in a high density regime, the damping effects of the RF wave by fusion particles, and the low efficiency for driving the current (large recirculation power). These problems can be removed by inductive current drive using an Ohmic transformer and the quasi-continuous alternating current (AC) operation mode with a thermal and electric energy storage unit to provide a continuous electric power output. Inductive current drive has been so far the most reliable, simple and efficient method, and complicated physics is not expected in the ignited regime. Fish scales on the first wall for the synchrotron current drive, which plays a special role in the D-<sup>3</sup>He tokamak, are not needed, facilitating a simple structure of the first wall.

The disadvantage of the thermal fatigue of the first wall may be addressed by employment of coolant flow control where, during the rampdown and up phase, the coolant flow in the first wall is reduced, so that the temperature in the first wall may be kept constant. Mechanical fatigue problems of toroidal coils by an oscillating out-of-plane load can also be alleviated by long pulse operation for many hours. Thus an AC scheme can become a basic operation scenario in a D-<sup>3</sup>He tokamak fusion reactor, and a non-inductive current drive scheme can be a back up or auxiliary system for controlling the plasma current profile if it is needed.

The first experiment on AC operation has been achieved in the small STOR-1M tokamak [1] and AC experiments in a large machine have been recently demonstrated in JET [2]. An AC tokamak reactor (ACTR) has been proposed for D-T fuels based on these experimental results [3].

In this paper, we propose an AC operated D-<sup>3</sup>He tokamak reactor with a small current drive power and a simple first wall structure, and consider what condition and machine size are necessary to have AC operation.

## 2. Flux Condition for AC Tokamak Operation

An AC tokamak must satisfy "the flux condition for AC operation" [3], to achieve AC operation with a one cycle pulse length ( $2T_{AC}$ ) longer than that of single swing operation ( $T_1$ ). The total

transformer flux ( $\Phi_t$ ) available in the tokamak must be larger than the inductive flux ( $\Phi_L$ ) by a factor of three,  $\Phi_t/3 > \Phi_L$ . More precise flux condition for AC operation is given by

$$\Phi_t/3 > (\Phi_L - \Phi_R/3), \quad (1)$$

where  $\Phi_R$  is the resistive flux during the current ramp-up and ramp-down phase given by  $\Phi_R \sim 0.4 \mu_0 R I_p$ . This condition favors a high aspect ratio with a large major radius, because a larger transformer flux can be employed.

It is difficult to satisfy this condition in the D-<sup>3</sup>He tokamak reactor because the plasma current and the inductive flux are larger than that in the D-T tokamak reactor. Therefore, the machine size optimization has to be done carefully to achieve AC operation in the D-<sup>3</sup>He tokamak reactor. The Ohmic transformer radius is calculated by

$$R_{OH} = R - a - \Delta_{gl} - \Delta_{sh} - \Delta_{tr} - \Delta_{bc} - \Delta_{oh} \quad (2)$$

where  $\Delta_{gl}$  is the scrape-off layer thickness,  $\Delta_{sh}$  is the thickness of the shield,  $\Delta_{tr}$  is the width of the toroidal coil,  $\Delta_{bc}$  is the width of the backing cylinder for the toroidal coil radial movement protection, and  $\Delta_{oh}$  is the half thickness of the Ohmic transformer coil. The total transformer flux is then given by

$$\Phi_t = 2\pi R_{OH}^2 B_{OH} + \Phi_{VE}, \quad (3)$$

where  $B_{OH}$  is the maximum magnetic field in the transformer solenoid coil,  $\Phi_{VE}$  is the flux contribution from the outer vertical equilibrium-coils, which is about 300 Vsec for  $I_p \sim 50$  MA. In this calculation, we assume  $\Delta_{gl} = 0.1$  m,  $\Delta_{sh} = 0.7$  m,  $\Delta_{tr} = 1$  m,  $\Delta_{bc} = 0.5$  m, and  $\Delta_{oh} = 0.5$  m. The inductive flux is calculated by  $\Phi_L = I_p I_p = \mu_0 R I_p [\log(8R/(a l_k)) - \ell_1/2 - 2]$  with  $l_k^2 = [1 + \kappa^2(1 + 2\delta^2 - 1.2\delta^3)]/2$ ,  $\delta$  the plasma triangularity, and  $\kappa$  the plasma elongation.

From the flux relationship shown in Fig. 1 for the case of  $B_t = 10$  T,  $a = 2.8$  m,  $\kappa = 2$ ,  $\delta = 0.7$ ,  $q_a = 2.8$ , and  $\ell_1 = 1$ , we see that the critical major radius for AC operation is almost  $R = 9.5$  m corresponding to  $I_p = 53.6$  MA, where  $\Phi_t/3 > (\Phi_L - \Phi_R/3)$  is marginally satisfied for  $B_{OH} = 18$  T. Here we have  $R_{OH} = 3.9$  m,  $\Phi_t = 2020$  Vsec,  $\Phi_L = 739$  Vsec, and  $\Phi_R = 256$  Vsec. In the following we use

these machine parameters for a D-<sup>3</sup>He AC tokamak reactor.

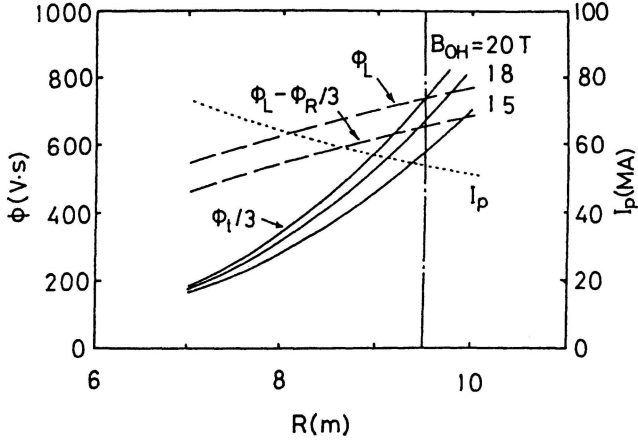


Fig.1 Flux relationship vs the major radius for  $a = 2.8$  m,  $\delta = 0.7$ ,  $\kappa = 2$ ,  $q_a = 2.8$ ,  $B_t = 10$  T, and  $\ell_i = 1$ .

### 3. Ignition Characteristics in the D-<sup>3</sup>He Tokamak Reactor

#### 3.1. Operation Path and Ignition Boundary.

The operation paths [4] for ITER89P, off-set linear (OL), and Goldston L-mode scalings with the confinement enhancement factor of  $\gamma_H = 4$ , and ITER92-H-P ELM free ( $\gamma_H = 1.15$ ) and ELMY ( $\gamma_H = 2$ ) H-mode scalings and the ignition boundary are shown in Fig. 2 for  $\bar{n}_e \sim 2.9 \times 10^{20} \text{ m}^{-3}$ . Here, ITER92-H-P ELM free and ELMY H-mode scalings [5] are given, respectively, by

$$\tau_{E,th} = \gamma_H 0.032 I_p^{0.95} B_t^{0.2} A_i^{0.45} R^{1.95} \kappa^{0.65} (a/R)^{0.05} \times n_e^{0.3} (\times 10^{19} \text{ m}^{-3}) / P_H^{0.65} \quad (4)$$

$$\tau_{E,th} = \gamma_H 0.034 I_p^{0.9} B_t^{0.05} A_i^{0.4} R^{2.1} \kappa^{0.8} (a/R)^{0.2} \times n_e^{0.3} (\times 10^{19} \text{ m}^{-3}) / P_H^{0.65} \quad (5)$$

The total net heating power  $P_H$  was replaced by  $P_{Ht} 2\pi^2 R a^2 \kappa$  for the analyses. The ignition regime exists for all scalings assumed here with the plasma parameters: the parabolic density and temperature profile  $\alpha_n = \alpha_T = 1$ , peak electron density  $n_e(0) = 4.3 \times 10^{20} \text{ m}^{-3}$ , the ion to electron temperature ratio  $T_i(0)/T_e(0) = 1.2$ , the 14 MeV proton confinement efficiency  $\eta_{p14} = 0.9$ , average impurity charge  $Z = 7$ , the effective ion charge  $Z_{eff} = 1.7$ , impurity fraction to the electron density  $f_z = 0.5\%$ , alpha and proton particle ash fraction to the electron density  $f_\alpha = f_p = 0.02$ , fuel density ratio of deuterium and <sup>3</sup>He  $n_D/n_{3HE} = 2$ , the hole fraction  $f_H = 0.1$  and wall reflectivity  $R_{eff} = 0.965$  for the synchrotron radiation loss [6]. The high confinement factor of  $\sim 4$  over ITER89P L-mode scaling may be a reasonable extrapolation from the V-H mode in DIII-D experiments [7]. H-mode scaling has to be further improved by up to a factor two to reach D-<sup>3</sup>He ignition as shown here. The mass factor is taken to be  $A_i = 2$  because <sup>3</sup>He fuels do not show any confinement improvement in JET [8].

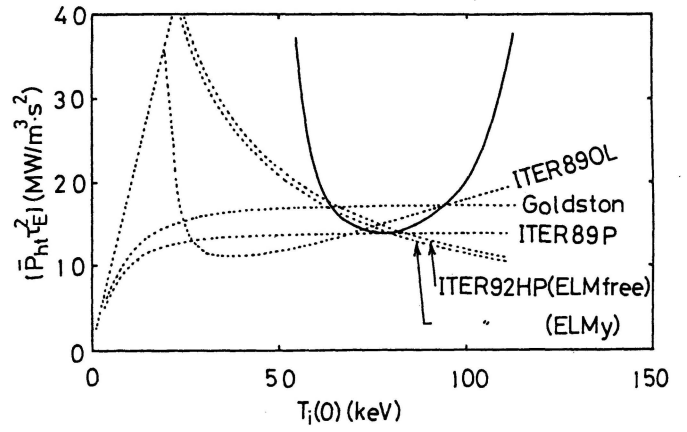


Fig.2 The operation paths of the D-<sup>3</sup>He tokamak reactor and the ignition boundary on the  $P_{Ht} \tau_E^2 - T_i$  plane. The parameters are  $\alpha_n = \alpha_T = 1$ ,  $n(0) = 4.3 \times 10^{20} \text{ m}^{-3}$ ,  $T_i(0)/T_e(0) = 1.2$ ,  $\eta_{p14} = 0.9$ ,  $Z = 7$ ,  $Z_{eff} = 1.7$ ,  $f_z = 0.5\%$ ,  $f_\alpha = f_p = 0.02$ ,  $f_D = 0.452$ ,  $f_{3He} = 0.226$ ,  $f_H = 0.1$  and  $R_{eff} = 0.965$ .

#### 3.2. Operating Point and Auxiliary Heating Power in POPCON

To have a fusion power  $\sim 3$  GW and a large bootstrap current, the operating point A as shown in Fig. 3 has been selected at  $n_e(0) = 4.3 \times 10^{20} \text{ m}^{-3}$  and  $T_i(0) \sim 75$  keV on the ignition boundary in POPCON for ITER89P scaling with  $\gamma_H = 4$ , where  $\beta_p \sim 1.62$  and  $T_e(0) \sim 62.5$  keV. The toroidal beta value  $\langle \beta_t \rangle_{op} \sim 6.5\%$  at the operating point is smaller than the Troyon beta limit  $\langle \beta_t \rangle_{TROY} = 3.5 I_p / a B_t \sim 6.7\%$ .

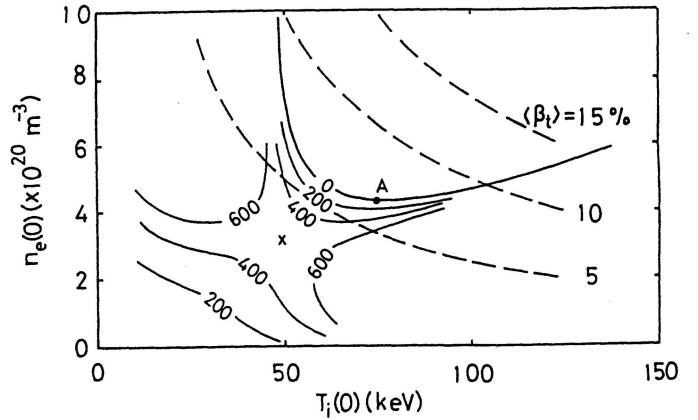


Fig.3 Operating point (A) in POPCON for ITER89P scaling with  $\gamma_H = 4$  in the D-<sup>3</sup>He tokamak reactor.

The actual fusion power is  $P_f \sim 3.7$  GW, where the bremsstrahlung loss is  $P_b \sim 1.4$  GW, the synchrotron radiation loss is  $P_s \sim 1.5$  GW, and the plasma conduction loss is  $P_L \sim 0.8$  GW. The electric power output from thermal conversion due to the bremsstrahlung and synchrotron radiation losses may be  $P_{e,b} \sim 880$  MW for the conversion

efficiency of 40 %, and the one by the rectenna conversion of the synchrotron radiation is  $P_{e,s} \sim 360$  MW for the waveguide loss of 20 % and conversion efficiency of 80 %. The thermal wall loading is  $(P_b + P_s)/S_{wall} \sim 1.4$  MW/m<sup>2</sup>, and the divertor heat load is  $P_L/S_{div} \sim 27$  MW/m<sup>2</sup> with a 0.5 m wide divertor target plate.

The auxiliary heating power  $P_H$  is rather large,  $\sim 475$  MW for  $T_i(0)/T_e(0) = 1.2$ . To reduce the heating power, we examine the effect of spin polarization of D and <sup>3</sup>He ions on the 50 % fusion reactivity enhancement ( $\gamma_{spin} = 1.5$ ), and hot ion mode operation as shown in Fig. 4.

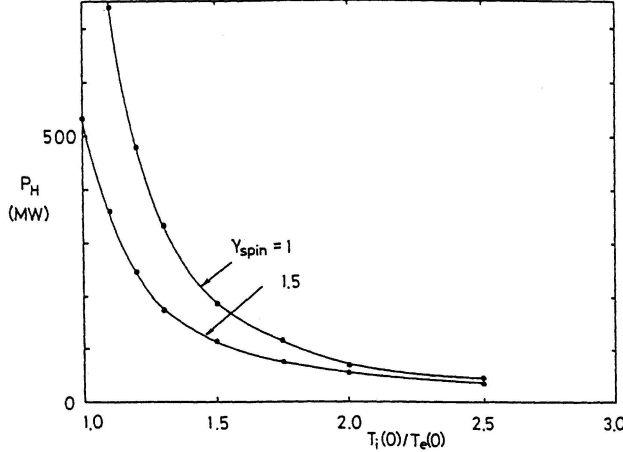


Fig.4 Dependence of minimum auxiliary heating power on the hot ion mode operation, and spin polarization effect for ITER89P scaling with  $\gamma_H = 4$ . ( $q_a = 2.8$ ).

It is found that the heating power to reach ignition is sensitive to the ion to electron temperature ratio  $T_i(0)/T_e(0)$ ; for example  $P_H \sim 70$  MW for the hot ion mode of  $T_i(0)/T_e(0) = 2$  and unpolarization ( $\gamma_{spin} = 1.0$ ). Spin polarization is especially effective in reducing the heating power in the regime with a low ion to electron temperature ratio; for example, spin polarization ( $\gamma_{spin} = 1.5$ ) yields  $P_H \sim 245$  MW for  $T_i(0)/T_e(0) = 1.2$ .

Low toroidal field operation decreases the synchrotron radiation, and therefore it can reduce the heating power. The minimum heating power is 340 MW at  $B_t = 7$  to 7.5 T for  $T_i(0)/T_e(0) = 1.2$  and  $\gamma_{spin} = 1.0$  as shown in Fig.5, where the plasma current is proportional to the toroidal field for the same safety factor and plasma shape parameters. Combination with spin polarization further reduces the heating power to 120 MW. In the current startup phase this operation scenario may be employed, and the toroidal field can be increased after passing the saddle point in POPCON, and then ignition can be reached in the first stability regime with enhanced synchrotron radiation losses.

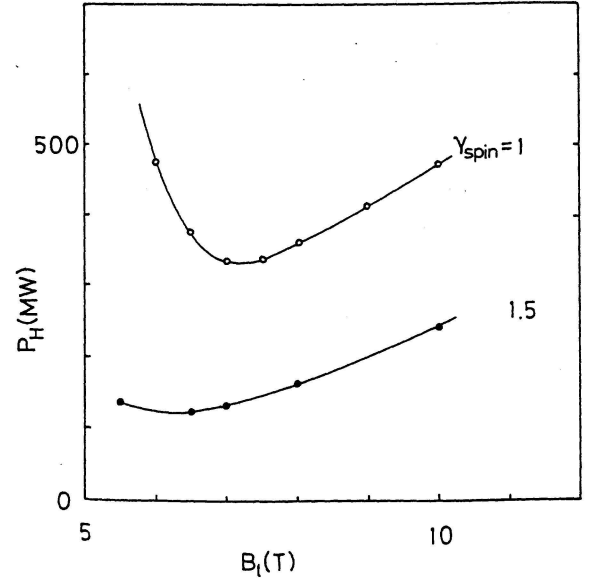


Fig.5 Dependence of minimum auxiliary heating power on the toroidal field and spin polarization effect for ITER89P scaling with  $\gamma_H = 4$ . ( $q_a = 2.8$ )

#### 4. AC Operation with Large Bootstrap Current Fraction

At the operating point (A) on Fig. 3, the neoclassical plasma resistance is  $R_{NC} = 0.77$  n $\Omega$  for  $T_e(0) = 62.5$  keV, therefore the loop voltage is  $V_{loop} = R_{NC}(1 - I_{BS}/I_p)I_p = 9.8$  mV for  $I_{BS}/I_p = 76$  % at  $\beta_p = 1.62$ . Here, the bootstrap current fraction is given by [9]

$$I_{BS}/I_p = \sqrt{\frac{a}{R}} \kappa \beta_p Q_\alpha 0.0673 \left\{ \frac{1}{\alpha_n + \alpha_T - 0.421} - \left(1 - \frac{q(0)}{q_a}\right) \frac{1}{\alpha_n + \alpha_T + \gamma - 0.421} \right\}, \quad (6)$$

where  $\gamma = 0.3$  and  $Q_a = (\alpha_n + \alpha_T + 1)(9.64\alpha_n + 0.642\alpha_T)$ , which provides a smaller bootstrap current fraction than ITER scaling [10]. The current drive power in the plasma side is therefore quite small,  $P_{CD} = V_{loop}I_p \sim 0.53$  MW. The power for driving the transformer action ( $P_{CD,T}$ ) can be estimated by the time derivative of the stored energy in the transformer ( $W_{OH}$ ) to be as small as  $P_{CD,T} = d(W_{OH})/dt \sim 1.9$  MW. Compared to this value, the **non-inductive current drive method needs a prohibitively large current drive power**. For example, for a non-inductive current drive efficiency  $\eta_{CD} = R \bar{n}_e I_p (1 - I_{BS}/I_p)/P_{CD} \sim 1 \times 10^{20}$  A/Wm<sup>2</sup>, which is assumed to be almost the double of the presently obtained maximum value, the current drive power is  $P_{CD} \sim 350$  MW in the plasma side for driving the same plasma current of  $I_p = 53.6$  MA with a high density plasma of  $\bar{n}_e = 2.9 \times 10^{20}$  m<sup>-3</sup> and the high bootstrap current fraction of  $I_{BS}/I_p = 76$  %. Therefore, the operational power of the non-inductive current drive system is about **700 MW** for a conversion of

efficiency of 50 %, resulting in a very small net electric power output from the fusion plant.

The first positive pulse length is  $T_1 = (\Phi_t - \Phi_L - \Phi_R) / V_{loop} \sim 29$  hours, and the subsequent AC pulse lengths are  $T_{AC} = (\Phi_t - 2\Phi_L) / V_{loop} \sim 15$  hours. In Fig.6, we show the numerically calculated AC current waveform in the D-<sup>3</sup>He tokamak. It is seen that the first pulse is almost twice of the subsequent AC pulse.

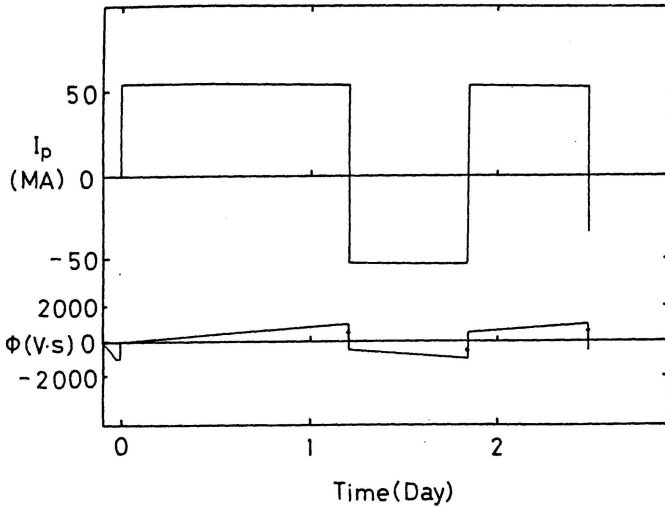


Fig.6 AC current waveform and flux variation of the transformer in the proposed D-<sup>3</sup>He AC tokamak reactor.

We have surveyed more parameters of the D-<sup>3</sup>He AC tokamak reactors as listed in Table 1.

## 5. Summary

We have presented the AC operated D-<sup>3</sup>He tokamak reactor with the parameter of  $R = 9.5$  m,  $a = 2.8$  m,  $B_t = 10$  T,  $\delta = 0.7$ ,  $\kappa = 2$ ,  $q_a = 2.8$ ,  $I_p = 53.6$  MA and more than 15 hours AC pulse length. The inductive current drive power is only 500 kW in the plasma side and 1.9 MW in the transformer side, which is more than three hundred times smaller than the non-inductive drive method. The auxiliary heating power to reach ignition is rather large  $\sim 475$  MW for  $T_i(0)/T_e(0) = 1.2$ . Spin polarization, hot ion mode operation and low toroidal field operation in the current startup phase may reduce the heating power further.

Thus an "advanced inductive operation" such as an AC operation mode with the high bootstrap current fraction may be the only one solution for driving the large plasma current with high density in a D-<sup>3</sup>He tokamak fusion reactor, and a non-inductive current drive scheme can serve an auxiliary system for controlling the plasma current profile.

Table 1. Machine parameters for the proposed D-<sup>3</sup>He AC tokamak reactor with  $T_i(0)/T_e(0) = 1.2$ .  $B_{OH} = 18$  T and  $\Phi_{VE} = 300$  Vsec are used. The height of the operation path  $[P_{h,net}\tau_E^2]_{op}$  is calculated using ITER89P scaling with  $\gamma_H = 4$ .

Reactor		DHETR-9.5		
R	(m)	9.5		
a	(m)	2.8		
$q_a$		2.8	2.8	2.6
$\delta$		0.5	0.7	0.7
$I_p$	(MA)	47.1	53.6	57.7
$\gamma_H$		4.5	4.0	4.0
$n_e(0)$	( $\times 10^{20} m^{-3}$ )	4.32	4.30	4.20
$T_i(0)$	(keV)	75	75	75
$P_f$	(GW)	3.75	3.7	3.6
$[P_{h,net}\tau_E^2]_{op}$	(MW/m <sup>3</sup> s <sup>2</sup> )	15.1	14.9	16.9
AC Capability		AC	AC	AC
$R_{OH}$	(m)	3.9		
$\Phi_t$	(Vsec)	2020		
$\Phi_L$	(Vsec)	686	739	796
$R_{NC}$	(n $\Omega$ )	0.77	0.77	0.77
$\beta_p$		1.85	1.62	1.45
$I_{BS}/I_p$		0.87	0.76	0.68
$V_{loop}$	(mV)	4.7	9.8	14
$T_1$	(h)	65	29	18
$T_{AC}$	(h)	38	15	8.5
$\langle \beta_t \rangle_{op}$	(%)	6.5	6.5	6.4
$\langle \beta_t \rangle_{TROY}$	(%)	5.8	6.7	7.2

## Reference

- [1] O. MITARAI, et al., Bull. Am. Phys. Soc., 29, (1984) 1337, Nucl. Fusion, 27, (1987) 604, and Nucl. Fusion, 32, (1992) 1801.
- [2] B. TUBBING, et al., Nuclear Fusion, 32, (1992) 967.
- [3] O. MITARAI, et al., Fusion Technology, 15, (1989) 204, and Fusion Technology, 20, (1991) 285.
- [4] O. MITARAI, et al., Fusion Technology, 22, (1992) 227.
- [5] O.J.W.F. KARDAUN, et al., in 13th International Conference on Plasma Physics and Controlled Nuclear Fusion Research, IAEA-CN-56/F-1-3 (Würzburg, Germany, Sep., 1992).
- [6] O. MITARAI, et al., Fusion Technology, 19, (1991) 234, and Fusion Technology, 21, (1992) 2265.
- [7] G.L. JACKSON, et al., Phys. Rev. Lett., 67, (1991) 3098.
- [8] JET JOINT UNDERTAKING, Progress Report, 1991, Vol.1, 104.
- [9] K. OKANO, Kakuyugo Kenkyu, 68, (1992) 404.
- [10] H.R. WILSON, Nuclear Fusion, 32, (1992) 257.